A contactless method for measuring amplitude and phase of RF voltages up to 26.5 GHz

Mathias Poik, Thomas Hackl, Stefano Di Martino, Bernhard M. Berger, Sebastian W. Sattler and Georg Schitter

***Abstract*—In this paper, a method for contactless amplitude and phase measurements of local voltages within microwave devices is developed. A conductive cantilever probe with a sharp tip is used as capacitively coupled sensor to record radio frequency (RF) voltages at well-defined distances between the probe tip and the device surface. The recorded voltage is compared to a nonlinear capacitance vs. distance model to separate the local voltage on the device from long-range cross-talk contributions. To determine both amplitude and phase of the local voltage, a complex parameter identification procedure is proposed and implemented. Thus, amplitude and phase measurements of local voltages at µm spatial resolution are enabled. Additionally, the cantilever probe is integrated on a PCB to enable the transmission of RF signals from the tip to the detector over a wide bandwidth. The proposed method, together with the developed probe, are verified by performing voltage measurements on an open-ended transmission line at frequencies from 1 GHz to 26.5 GHz. The measurements closely match the analytically calculated standing wave patterns on the transmission line.**

***Index Terms*— RF sensing, contactless voltage measurement, phase measurement, wide bandwidth, voltage probe**

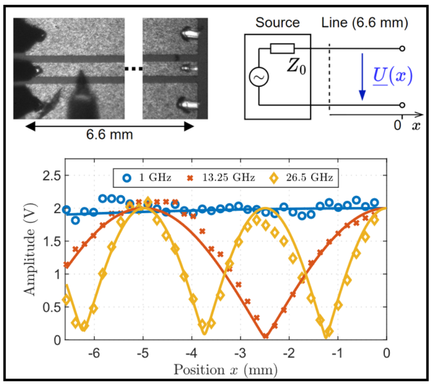

Contactless RF sensing at frequencies up to 26.5 GHz, closely matching calculated standing wave patterns.

I. Introduction

The ongoing miniaturization along with a shift towards higher frequencies poses a significant challenge for the characterization of microwave circuits and devices. Conventional contact-based probing techniques can measure only the input-output behavior of devices and require relatively large contact pads with typical sizes of 50 µm to 100 µm [1]. The contact pads can even be significantly larger than individual circuit blocks or interconnections between blocks, which have dimensions down to a few µm. This inherently limits access to relevant internal voltages, whose knowledge would aid the development of these devices. For instance, the voltage distribution within large active area devices such as antenna switches [2] or power amplifiers [3] can show significant non-linearities due to parasitic capacitances to the device substrate. Although device properties can be inferred from contact-based measurements at the input and output [4], this approach is limited by the complexity of the used model. It is also possible to integrate RF detectors on the chip and thus obtain local voltages within the device [5]. However, these detectors occupy precious chip area, especially when both RF amplitudes and phases need to be measured, since this requires the integration of relatively large circuit blocks such as six-port reflectometers [6]. A direct measurement of amplitude and phase of local RF voltages with µm spatial resolution would therefore greatly benefit the future development of miniaturized microwave devices.

Passive voltage probes have been widely used for contactless measurements of local RF voltages [7]–[9]. They typically consist of an open-ended transmission line (e.g. open coaxial cable) with a miniaturized tip which is placed vertically over the circuit (i.e. perpendicular to the surface). The tip capacitively couples to a test point on the circuit and the RF signal is transmitted to a vector network analyser (VNA). No ohmic contact is needed, enabling localized measurements of RF voltages within microwave devices at high spatial resolution. For instance, passive voltage probes have been used for contactless measurements of RF voltages with frequencies up to 8 GHz at individual drain/source electrodes of power amplifiers with 70 µm separation [10].

The achievable spatial resolution of the voltage measurement is mainly limited by the size of the tip as well as by cross-talk from adjacent circuit parts [11]. Probes with miniaturized tips have been developed to achieve a high spatial resolution [12]. Additionally, the voltage is typically obtained in a differential procedure by subtracting two measurements at different tip-surface distances [13]. Since the gradient of the

M. Poik, T. Hackl, and G. Schitter are with the Automation and Control Institute (ACIN), TU Wien, Gusshausstrasse 27-29, 1040 Vienna, Austria (email: poik@acin.tuwien.ac.at).
S. Di Martino, B. M. Berger and S. W. Sattler are with Infineon Technologies Austria AG, Austria.
The financial support by the FFG Production of the Future programme (Project Nr. 883916) of the Austrian BMK is gratefully acknowledged.

tip-circuit capacitance is highest for circuit elements closest to the tip, the subtraction enables a reduction of cross-talk from adjacent circuit parts. A drawback of this method is that computing the difference between measurements at different distances results in a reduced sensitivity, leading to a trade-off between spatial resolution and sensitivity. Resonant probes have been designed to improve the sensitivity within narrow frequency bands [14]. However, these probes are limited to applications where the investigated device is operated at the respective frequency band.

For characterising broadband microwave devices, such as switches and amplifiers, voltage probes need to be capable of detecting signals over a wide bandwidth of RF frequencies. Recently, several wide bandwidth probes have been constructed out of PCBs made of low-loss materials, where the tip is implemented directly on the PCB as short protruding trace of transmission lines, such as striplines or coplanar waveguides [15], [16]. With these designs, voltage and current probes with a wide bandwidth of up to 26 GHz have been achieved [17], [18]. A drawback of the direct integration of the tip on a PCB is that the minimum achievable tip size is limited by design rules to tens or hundreds of µm. Additionally, it is difficult to precisely measure and control the distance between the PCB and the device and thus the tip-surface distance. These limitations resulted in an achievable spatial resolution of hundreds of µm so far.

In contrast to the described vertical and PCB-based probe designs, cantilever probes which are commonly used in Atomic Force Microscopy (AFM) [19] and Scanning Microwave Microscopy (SMM) [20] enable a precise detection of mechanical contact between tip and surface. It has been shown that a cantilever probe with a sharp tip allows contactless RF voltage measurements at multiple well-known tip-surface distances [21]. By comparing the results to an analytic capacitance vs. distance model the previously mentioned trade-off between spatial resolution and sensitivity can be overcome, thus enabling RF voltage measurements at spatial resolutions $< 2\,\mu m$ [22]. However, the method in [21] has only been formulated and verified for voltage amplitude measurements. Additionally, due to reflections in the RF signal path the achievable bandwidth of the probe was limited and measurements were demonstrated only up to 13 GHz. Existing methods therefore do not enable contactless voltage amplitude and phase measurements with the µm spatial resolution necessary for characterizing integrated microwave devices.

The contribution of this paper is a model-based method for amplitude and phase measurements of RF voltages at µm spatial resolution over a wide bandwidth of 1 GHz to 26.5 GHz. Contactless voltage measurements at high spatial resolution are achieved by using a capacitively coupled cantilever probe with a sharp tip and performing measurements at well-defined tip-surface distances. To account for cross-talk induced measurement errors, the model-based method presented in [21] is generalized and extended to enable both amplitude and phase measurements of the local RF voltage. Additionally, a passive voltage probe for wide-bandwidth transmission of RF signals from the probe tip to the detector is developed. The proposed method together with the developed voltage probe are verified by performing RF voltage measurements of standing waves on an open-ended transmission line at frequencies from 1 GHz up to 26.5 GHz.

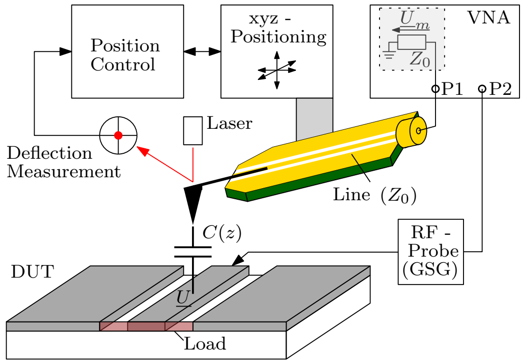

Fig. 1: Block diagram of RF sensing system. Adapted from [21].

II. Probe description

Fig. 1 illustrates the working principle of the implemented RF sensing system [21]. A conductive probe with a sharp tip is positioned close to the surface and couples via the capacitance $C(z)$ to the device under test (DUT) to measure the local RF voltage $\underline{U}$. The DUT can be a microwave circuit with test points or traces on the surface or close to the surface (e.g. beneath a thin passivation layer). The probe is connected to a transmission line which itself is connected to a VNA. In a simplified approximation, the RF sensing system can be modelled as a series connection between the tip-circuit capacitance and the impedance of the transmission line. The voltage measured by the VNA can therefore be modelled as

$$\underline{U}_\mathrm{m} = \underline{U} \cdot \frac{j\omega Z_0 C}{1 + j\omega Z_0 C} \approx \underline{U} \cdot j\omega Z_0 C \,, \quad (1)$$

where ω, and $Z_0 = 50\,\Omega$ denote the circular frequency and the characteristic impedance, respectively. The approximation in (1) is valid for low tip-circuit capacitances $C \ll \frac{1}{\omega Z_0}$.

A. Requirements for wide-bandwidth voltage probe

In (1) it is assumed that the probe is electrically short and provides a direct electrical connection between the capacitance $C(z)$ and the input of the transmission line. This quasi-static assumption is valid if the length of the protruding probe is significantly smaller than the wavelength λ of the respective RF signal [23]. If the length approaches $\lambda/4$ the probe acts as an antenna and shows resonances in the transfer function, which inherently attenuate the signal coupled onto the transmission line. For maximizing the bandwidth the protruding probe should therefore be as short as possible.

A conflicting design consideration is the clearance of the transmission line to parts of the DUT. The DUT is typically connected to evaluation boards or other measurement equipment by bond wires with loop heights of tens of µm, or by RF-probes that contact the pads on the DUT. For access to

Published version of the article: Mathias Poik, Thomas Hackl, Stefano Di Martino, Bernhard M. Berger, Sebastian W. Sattler and Georg Schitter, "A contactless method for measuring amplitude and phase of RF voltages up to 26.5 GHz ", *IEEE Sensors Journal*, 2024. DOI: 10.1109/JSEN.2024.3354322

This article has been accepted for publication in IEEE Sensors Journal. This is the author's version which has not been fully edited and content may change prior to final publication. Citation information: DOI 10.1109/JSEN.2024.3354322

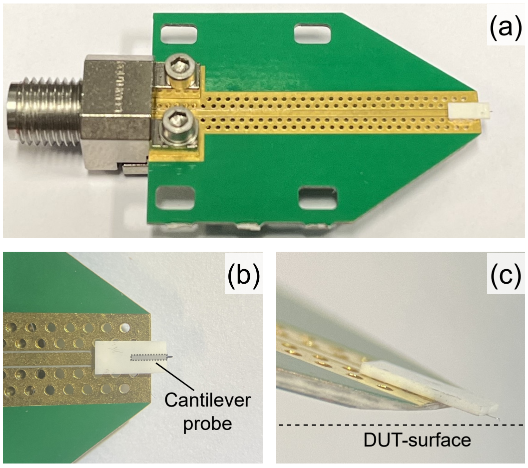

Fig. 2: (a) PCB with the probe substrate mounted at the end of the transmission line. (b)-(c) Close-up of the mounted probe. The end of the PCB is flattened such that the tip is the lowest point and can reach the sample surface.

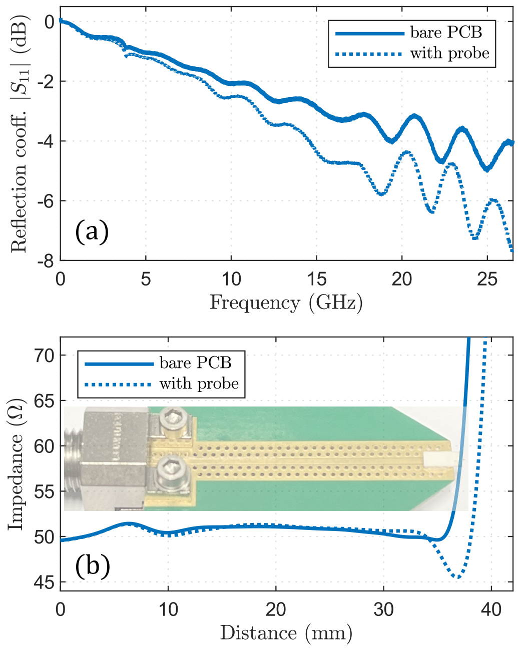

Fig. 3: Measurement of (a) reflection coefficient and (b) impedance of the PCB with and without mounted cantilever probe.

circuit parts close to bond wires or RF-probes, the probe needs a sufficiently high aspect ratio, i.e. the relatively large transmission line in Fig. 1 must be sufficiently far away from the DUT.

The coupling capacitance C and thus the measurement sensitivity strongly depends on the tip-surface distance z. Additionally, unwanted coupling capacitances to other circuit parts have to be compensated by a suitable measurement procedure to enable voltage measurements with high spatial resolution. The RF sensing system must therefore be capable of measuring the voltage at well-defined tip-surface distances. This can be achieved by using a cantilever probe together with an optical deflection measurement, which are commonly employed in AFM and enable a precise detection of mechanical tip-surface contact. In combination with a high precision positioning system, this enables RF voltage measurements at well-defined tip-surface distances.

B. Probe implementation

A micro-machined cantilever probe (25Pt300C, Rocky Mountain Nanotechnology, USA) which is commonly employed in electrical AFM measurement modes is used in this work. The cantilever has a length of 300 µm with a sharp tip of 100 µm length and an apex radius smaller than 100 nm at its end. To meet the requirement for an electrically short probe protrusion, the cantilever is mounted directly to the end of an open-ended transmission line on a PCB. A grounded coplanar waveguide (GCPW) with a length of 30 mm is implemented on a low-loss substrate (Rogers4003C) with a thickness of 0.41 mm. It is designed for a characteristic impedance of 50 Ω and is connected to a VNA by a 2.92 mm adapter. The cantilever probe is manually attached to the open end of the GCPW. Fig. 2 shows photographs of the implemented PCB with the mounted cantilever probe substrate (white rectangle).

To ensure the tip can access the surface of the DUT (i.e. to ensure the tip is vertically the lowest point of the probe), the end of the PCB is flattened as shown in Fig. 2c. In this implementation, the cantilever probe protrudes the transmission line by about 1.5 mm. For this length, resonances in the transfer function are expected if the frequency approaches $\frac{c_0}{4 \cdot 1.5\,\mathrm{mm}} = 49.8\,\mathrm{GHz}$, which is well above the maximum frequency range of 26.5 GHz considered in this work. However, due to the flattening of the end of the PCB as well as due to the presence of the probe substrate, the transmission line impedance is altered on the last millimeters of the PCB. To determine the impact of this, the reflection coefficient of the probe PCB is analysed.

C. Analysis of reflection coefficient

The reflection coefficient of the probe PCB is measured by a VNA (ZNA26, Rohde & Schwarz, Germany). The VNA is connected to the PCB by a coaxial cable and the calibration reference plane is at the end of the cable. For the analysis the bare PCB (i.e. before flattening and mounting the probe) is compared to the final implemented probe PCB.

Fig. 3a shows the measured reflection coefficient S_{11}. The results show the frequency dependent damping of the 30 mm long PCB, as well as ripples due to reflections between the open end and the 2.92 mm connector. Flattening the end of the PCB and mounting the probe leads to an increased damping in the measured S_{11} at higher frequencies. No distinct resonance peaks are introduced in the considered frequency range, which

Published version of the article: Mathias Poik, Thomas Hackl, Stefano Di Martino, Bernhard M. Berger, Sebastian W. Sattler and Georg Schitter, "A contactless method for measuring amplitude and phase of RF voltages up to 26.5 GHz ", *IEEE Sensors Journal*, 2024. DOI: 10.1109/JSEN.2024.3354322

This article has been accepted for publication in IEEE Sensors Journal. This is the author's version which has not been fully edited and content may change prior to final publication. Citation information: DOI 10.1109/JSEN.2024.3354322

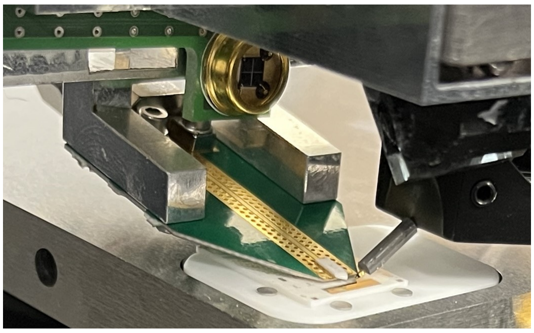

Fig. 4: Photograph of the experimental setup.

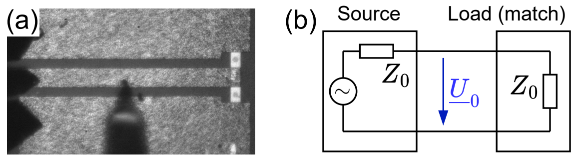

Fig. 5: (a) Microscope image of tip placed over matched line (length 550 µm). (b) Equivalent circuit of matched line. The RF voltage on the line is equal to the voltage $\underline{U}_0$ applied by the VNA via a RF-probe.

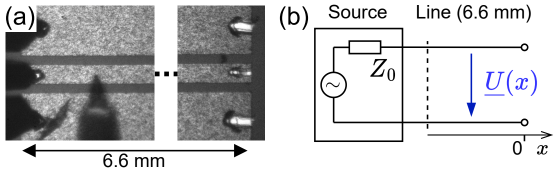

Fig. 6: (a) Microscope image of tip placed over long open-ended line (6.6 mm). The tip is moved along the line to record the RF voltage depending on the position. (b) Equivalent circuit of long open-ended line. The RF voltage $\underline{U}(x)$ varies depending on the position x.

indicates that the probe protrusion is sufficiently short. For a further analysis a step response time domain measurement is carried out and the resulting measured impedance along the PCB is shown in Fig. 3b. The results show the transition from the cable to the 50 Ω GCPW at about 7 mm. At 37 mm the bare PCB shows a steep increase, as expected for an open-ended line. With the mounted probe the impedance shows a small dip close to the end of the PCB, which may be explained by the increased capacitance due to the permittivity of the probe substrate. The steep increase of the impedance is shifted by about 2 mm, which can be explained by the increased length of the transmission line due to the protruding cantilever probe.

The analysis shows that the protruding cantilever probe introduces no significant resonances in the measured reflection coefficient, which indicates that the quasi-static assumption is valid and the probe can be considered an electrically short extension of the transmission line. It is therefore expected, that the developed probe enables contactless RF voltage measurements over a wide bandwidth according to (1).

III. Experimental Details and Device Under Test

The newly developed probe PCB is integrated in a custom-built AFM measurement head. Fig. 4 shows a photograph of the probe PCB mounted on an aluminium holder. The holder itself is mounted on a dual-stage positioning system, consisting of a piezo-based system for fine positioning and stepper motors for long-range movement. The fine positioning system consists of a piezo actuator with integrated strain gauges (PC4WMC2, Thorlabs, USA) for vertical probe movement and a two-axis piezo stage (NPXY100-100, nPoint, USA) for horizontal probe movement. The cantilever deflection is measured by an optical deflection measurement system. A laser is focused on the cantilever and the reflection is guided to a four-quadrant photo detector. As shown in Fig. 4, the cantilever is placed over a calibration substrate which is contacted by a RF-probe.

A. Device under test

Experiments are carried out on two different coplanar waveguide transmission lines on a RF calibration substrate (CS-5, Picoprobe). As shown in Fig. 5, the first transmission line is a matched line which is connected to the VNA via a ground-signal-ground (GSG) RF-probe. The microscope image in Fig. 5a shows the 550 µm long line with the RF-probe on the left side, and the match on the right side. Coming in from the bottom side of the image the cantilever probe and its tip can be seen placed several µm (vertically) above the center of the line for contactless voltage sensing. Fig. 5b shows an equivalent circuit of the matched line. Since the line is matched by its characteristic impedance, no reflections occur and the voltage on the line is equal to the voltage $\underline{U}_0$ applied via the RF-probe. The matched line with its well-defined voltage is therefore used as reference structure to evaluate the transfer function of the RF sensing system.

The second transmission line is a 6.6 mm long line which is left open at its end. Fig. 6a shows a microscope image of the line, which is connected to the VNA via a RF-probe on the left side. The open end can be seen on the right and the cantilever probe tip is again visible at the bottom side of the image. Fig. 6b shows an equivalent circuit of the open line. Due to reflections of RF signals from the open end, the voltage $\underline{U}(x)$ varies depending on the frequency and the horizontal position x. The expected voltage along the line equals

$$\underline{U}(x) = \underline{U}_0 \left(e^{-j\gamma x} + \Gamma e^{j\gamma x} \right) \,, \tag{2}$$

with the complex propagation constant $\gamma = \alpha + j\beta$ and the reflection coefficient Γ of the open end. The fringing capacitance at the open end leads to an effective length extension which can be approximated using the conductor width $w = 50\,\mu\text{m}$ and the gap $s = 25\,\mu\text{m}$ of the coplanar waveguide as $\Delta l \approx \frac{w+2s}{4} = 25\,\mu\text{m}$ [24]. With the phase velocity $c = 0.442 \cdot c_0$ as specified in the data sheet and the resulting wavelength of $\lambda = c/f$ this leads to a phase shift of only $360 \cdot \Delta l/\lambda = 1.8$ deg at 26.5 GHz. The fringe capacitance is therefore considered negligible and an ideal open end with a reflection coefficient of $\Gamma = 1$ is assumed in this work.

Published version of the article: Mathias Poik, Thomas Hackl, Stefano Di Martino, Bernhard M. Berger, Sebastian W. Sattler and Georg Schitter, "A contactless method for measuring amplitude and phase of RF voltages up to 26.5 GHz ", *IEEE Sensors Journal*, 2024. DOI: 10.1109/JSEN.2024.3354322

This article has been accepted for publication in IEEE Sensors Journal. This is the author's version which has not been fully edited and content may change prior to final publication. Citation information: DOI 10.1109/JSEN.2024.3354322

The cantilever probe tip is horizontally moved along the line to measure the RF voltage depending on the position x at different frequencies. Due to the superposition of forward and backward travelling RF signals in (2), the 6.6 mm long open line provides significant amplitude and phase contrast within the relevant frequency range of 1 GHz to 26.5 GHz. This should enable a clear verification of the voltage amplitude and phase measurement capability of the implemented RF sensing system.

The microscope images in Fig. 5a and Fig. 6a show that the tip can be placed directly next to a RF-probe. This demonstrates, that the cantilever probe protrusion from the PCB transmission line as described in Section II leads to sufficient clearance between the relatively large PCB and the RF-probe. However, the protrusion of the unshielded cantilever probe could lead to cross-talk induced measurement errors. Considering Fig. 6a, it is for instance clear that there is significant unwanted capacitive coupling between the cantilever probe tip and the center pin of the RF-probe, which has to be compensated by a suitable measurement procedure.

IV. Model-based RF sensing for amplitude and phase measurements

A model-based measurement procedure is employed to compensate for cross-talk induced errors by performing multiple measurements at different tip-surface distances and identifying the local tip-circuit capacitance. The measurement procedure is described in detail in [21] for amplitude measurements and is generalized in this work to provide both amplitude and phase voltage measurements.

The capacitance between a cantilever probe and an electrode on the surface of the DUT can be separated in a long-range linear distance dependence and a short-range non-linear distance dependence [25]:

$$C(z) = \underbrace{C_{\mathrm{nl}}(z)}_{\text{short-range}} + \underbrace{C_{\mathrm{lin}}(z)}_{\text{long-range}}, \tag{3}$$

where z denotes the tip-surface distance. The non-linear part in (3) can generally be modelled by a logarithmic distance dependence [25]

$$C_{\mathrm{nl}}(z) = C_0 \cdot \ln\left(1 + \frac{R_{\mathrm{eff}}}{z}\right), \tag{4}$$

where C_0 is a constant capacitance and R_{eff} is an effective tip radius, which incorporates the shape and size of the tip apex. It can be seen from (4) that the non-linear part becomes significant only for small distances z in the order of the tip apex size. Unwanted coupling capacitances between the cantilever probe and circuit parts at a larger distance from the tip are therefore assumed to have a purely linear distance dependence $C_{\mathrm{lin}}(z) = a \cdot z + b$, with constants a and b. For a given frequency, the total voltage measured by the VNA according to (1) can therefore be separated in a short-range and a long-range part as well:

$$\underline{U}_{\mathrm{m}}(z) \propto \underbrace{\underline{U} \cdot C_{\mathrm{nl}}(z)}_{\text{short-range}} + \underbrace{\underline{U}_{\mathrm{lin}} \cdot C_{\mathrm{lin}}(z)}_{\text{long-range}}. \tag{5}$$

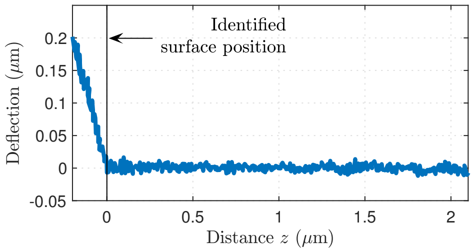

Fig. 7: Measured cantilever deflection during tip-surface approach and identified surface position.

The short-range part denotes the influence of the local tip-circuit capacitance C_{nl}. Since it is assumed that only the capacitance between the cantilever probe tip and circuit parts close to the tip apex has a non-linear distance dependence, the short-range part corresponds to the local voltage $\underline{U}$ at the tip position. In contrast, the long-range part combines all cross-talk contributions from circuit elements at a larger distance from the tip. In reality the total cross-talk consists of a superposition of contributions from multiple circuit locations with different voltages and coupling capacitances. However, since it is assumed that these contributions have a linear distance dependence, they can be combined into a single voltage $\underline{U}_{\mathrm{lin}}$.

Cross-talk can be eliminated by identifying $\underline{U}$ in (5). The long-range contributions combined in $\underline{U}_{\mathrm{lin}}$ can have both a different amplitude and phase with respect to the local voltage $\underline{U}$. The measurement procedure therefore requires measuring the voltage $\underline{U}_{\mathrm{m}}$ at multiple tip-surface distances and performing a complex least squares fit to identify $\underline{U}$.

A. Measurement procedure

To demonstrate the measurement procedure, the voltage $\underline{U}_{\mathrm{m}}$ is recorded depending on the tip-surface distance at a fixed horizontal position x on the line in Fig. 6. This measurement is carried out at a frequency of 1 GHz, and a voltage $\underline{U}_0$ with an amplitude of 1 V (10 dBm) is applied. A ramp signal is applied to the vertical piezo actuator such that the tip approaches the surface with a constant velocity. As shown in Fig. 7, mechanical contact between the tip and the surface is detected by measuring the cantilever deflection. The tip-surface distance during the approach is calculated based on the identified position of mechanical contact and the measured position of the piezo actuator. For the voltage measurement described in the following, only distances $z > 100$ nm are considered. Although the procedure includes mechanical contact of the tip with the surface, the actual RF voltage measurement is therefore contactless.

Fig. 8a shows the complex voltage $\underline{U}_{\mathrm{m}}$ measured with respect to the distance z while the tip approaches the surface. The black line shows the identified model, which is fitted to the measurement data by a least squares estimation of $\underline{U}$ and $\underline{U}_{\mathrm{lin}}$ according to (4)-(5). For the model in (4), an effective tip radius of $R_{\mathrm{eff}} = 500$ nm is used since it provides the best fit to the measurement data. Projections of the 3-dimensional plot in

Published version of the article: Mathias Poik, Thomas Hackl, Stefano Di Martino, Bernhard M. Berger, Sebastian W. Sattler and Georg Schitter, "A contactless method for measuring amplitude and phase of RF voltages up to 26.5 GHz", *IEEE Sensors Journal*, 2024. DOI: 10.1109/JSEN.2024.3354322

This article has been accepted for publication in IEEE Sensors Journal. This is the author's version which has not been fully edited and content may change prior to final publication. Citation information: DOI 10.1109/JSEN.2024.3354322

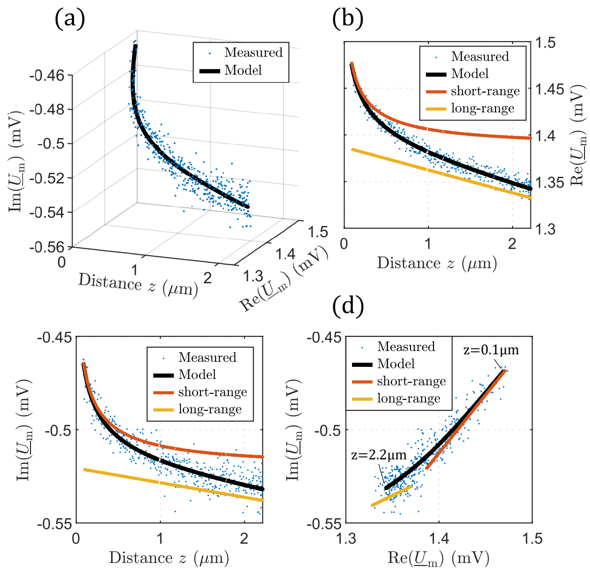

Fig. 8: Measured voltage $\underline{U}_\mathrm{m}$ depending on the tip-surface distance. (a) 3-dimensional plot of the complex voltage and the identified model. (b)-(d) Projections of the 3-dimensional plot depicting (b) real part vs. distance, (c) imaginary part vs. distance and (d) the complex voltage phasor.

Fig. 8a to the real and imaginary axes are depicted in Fig. 8b and 8c, respectively. Additionally, the short-range non-linear part and the long-range linear part according to (5) are shown. The identified voltage closely matches the measurement data which verifies the validity of the model and that the total voltage can be separated into a short-range non-linear part and a long-range linear part.

Fig. 8d depicts the projection to the complex plane, which shows the phasor of the voltage depending on the distance z. The identified short-range and long-range parts have different slopes, which indicates that the voltage $\underline{U}_\mathrm{lin}$, which contains all cross-talk contributions, has a different phase than the local voltage $\underline{U}$ at the tip position. Since the measured voltage $\underline{U}_\mathrm{m}$ is a weighted superposition of the short-range and long-range part, its phase varies and approaches that of the short-range part for smaller tip-surface distances z. According to the used model (5), the local voltage $\underline{U}$ is contained in the short-range part and can therefore directly be seen from the slope of the short-range part in Fig. 8d. The validity of this approach is analysed by measurements in Section VI.

The total measurement procedure involves the following steps:

- **Tip-surface approach**: The tip moves towards the surface while the tip position, the cantilever deflection and the voltage $\underline{U}_\mathrm{m}$ are measured.
- **Identification of surface position**: Mechanical contact with the surface is identified based on the cantilever deflection, which provides $\underline{U}_\mathrm{m}(z)$ at defined distances z.
- **Local voltage estimation by complex fit**: A complex fit is performed to identify the local voltage $\underline{U}$ according to the model (5).

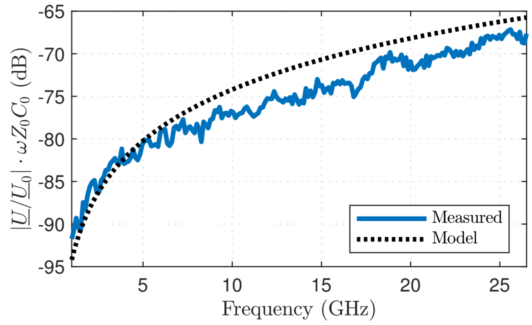

Fig. 9: (a) Measured transfer function from the applied voltage $\underline{U}_0$ to the identified local voltage $\underline{U}$.

The described procedure corresponds to the measurement of the voltage at one specific location on the DUT. Each curve is recorded within 0.1 s, i.e. the voltage on the DUT is measured at a data point rate of 10 Hz. To ensure that $\underline{U}_\mathrm{m}(z)$ can be correctly resolved during the tip-surface approach, the VNA intermediate frequency (IF) bandwidth is selected as 10 kHz, which is 1000 times higher than the data point rate. For the range of the tip-surface distance of 2.2 µm as shown in Fig. 8 this corresponds to recording $\underline{U}_\mathrm{m}(z)$ at a distance resolution of 2.2 nm.

V. Analysis of Measurement Bandwidth

To analyse the bandwidth of the RF sensing system, the cantilever probe tip is placed over the matched line as shown in Fig. 5a. The measurement procedure described in Section IV-A is carried out for different frequencies. Fig. 9 shows the measured transfer function from the applied voltage $\underline{U}_0$ to the identified local voltage $\underline{U}$. The transfer function increases with increasing frequency as expected from the simplified model in (1). According to the specifications of the calibration substrate, the coplanar lines are dispersive below a frequency of 5 GHz. The model in Fig. 9 is therefore normalized to the measured transfer function value at 5 GHz. For higher frequencies the deviation may be explained by damping of the probe PCB, which can also be seen in the reflection measurement in Fig. 3a. The small ripples in the transfer function can be explained by reflections due to imperfect transitions in the RF signal path from the tip via the probe PCB to the VNA. This could be improved by further optimizing the geometry of the probe PCB. However, no distinct resonances are visible in the measurement result which confirms that transmission of RF signals is possible over a wide bandwidth from 1 GHz to 26.5 GHz.

It can be seen from (4)-(5), that the voltage identified by the measurement procedure includes the unknown constant capacitance C_0, as well as the frequency dependence ωZ_0 from (1). The identified model in Fig. 9 corresponds to a parameter of $C_0 = 62$ aF.

Published version of the article: Mathias Poik, Thomas Hackl, Stefano Di Martino, Bernhard M. Berger, Sebastian W. Sattler and Georg Schitter, "A contactless method for measuring amplitude and phase of RF voltages up to 26.5 GHz ", *IEEE Sensors Journal*, 2024. DOI: 10.1109/JSEN.2024.3354322

A. Normalization for quantitative voltage measurements

Since the measurement and fitting procedure is identical for each measurement, the measured transfer function in Fig. 9 can be used for normalization to obtain quantitative results in subsequent RF sensing experiments. The prerequisite for obtaining quantitative results on a different DUT is that the local, non-linear part of the capacitance between the tip apex and the DUT remains the same. This is the case in this work, since both the transfer function measurement (on the matched line) and the measurements on the DUT (open line) are carried out in the center of relatively large conductors (line width $w \gg R_{\text{eff}}$). The identified transfer function can therefore be used for normalization to obtain quantitative voltage measurements along the open line in Fig. 6.

B. Probe intrusion and sensitivity

To ensure that the contactless RF sensing does not impact the actual voltage on the DUT, the measurement impedance must be significantly higher than the self-impedance of the circuit [10]. The measurement impedance is given by the capacitance between tip and DUT during the measurement. As described in Section IV-A, the minimum tip-surface distance during the voltage measurement is 100 nm and the effective tip radius is $R_{\text{eff}} = 500\,\text{nm}$. With the used model in (4) and the identified parameter of $C_0 = 62\,\text{aF}$, the maximum local capacitance between tip apex and the DUT therefore equals $C_{\text{nl}} = C_0 \ln(6) = 111\,\text{aF}$. For the frequency range from 1 GHz to 26.5 GHz used in this work, this corresponds to local measurement impedances $1/(\omega C_{\text{nl}})$ from $1.4\,\text{M}\Omega$ to $54\,\text{k}\Omega$. The identified values of the measurement impedance can be used to assess whether the contactless measurement is suitable (non-intrusive) for a given frequency, at a specific self-impedance level within a DUT. For the $50\,\Omega$ transmission line used in this work, the local measurement impedance is three orders of magnitude higher than the self-impedance. It is therefore expected that its influence on the voltage on the line is negligible (non-intrusive measurement). This assumption is analysed in Section VI by comparing the measured voltage with the analytically calculated voltage on the line.

Due to the low tip-circuit capacitance the signal levels at the VNA input port are 90 dB to 68 dB lower than on the DUT, as can be seen in Fig. 9. This measurement is carried out at a data point rate of 1 Hz (each recorded voltage vs. distance curve has a duration of 1 s) and a VNA intermediate frequency (IF) bandwidth of 1 kHz. The specified noise level at the VNA input port at an IF bandwidth of 1 kHz is 2.5 µV (-102 dBm). The achievable sensitivity of the measurement system can therefore be estimated as $79\,\text{mV}/\sqrt{\text{Hz}}$ (-12 dBm) to $6.3\,\text{mV}/\sqrt{\text{Hz}}$ (-34 dBm) for the frequency range of 1 GHz to 26.5 GHz. The estimated sensitivities are in agreement with the experimentally verified value of $20.1\,\text{mV}/\sqrt{\text{Hz}}$ at 13 GHz from [21].

VI. Measurement of RF voltage along transmission line

RF sensing experiments are performed along the open line from Fig. 6. A voltage with an amplitude of 1 V with different frequencies is applied by the RF-probe. The measurement procedure described in Section IV-A is carried out at multiple positions x on the line. At each position 200 measurements are carried out over an area of 5×5 µm and the resulting identified voltages are averaged. With a data point rate of 10 Hz this leads to a duration of 20 s per voltage measurement on a given position x on the line.

Fig. 10a shows the amplitude of the measured voltage along the line for frequencies of 1 GHz, 13.25 GHz and 26.5 GHz. The solid lines show the corresponding analytic calculation of the voltages according to (2). A phase constant $\beta = \omega/c$ with the phase velocity $c = 0.442 \cdot c_0$ is used as specified in the data sheet of the calibration substrate. The damping coefficient α is experimentally determined based on a transmission measurement of the line (data not shown). For a frequency of 1 GHz the 6.6 mm long line is electrically short and the amplitude of the voltage is therefore roughly constant along the line. Due to the reflection at the open end the amplitude has a value of 2 V, i.e. it is twice as high as the applied voltage amplitude. For 13.25 GHz and 26.5 GHz the superposition of forward and backward travelling RF signals and the resulting standing waves along the line can be seen. The distances between adjacent zeros correspond to half the wavelength $\lambda/2 = c/(2f)$ as expected. The measurement at 1 GHz appears more noisy than the results for 13.25 GHz and 26.5 GHz. This can be explained by the frequency dependent sensitivity of the measurement system, which leads to an improved signal-to-noise ratio at higher frequencies.

Fig. 10b shows the measured phase along the line. All phase measurements are referenced to the first data point at the beginning of the line. The results show the expected $180\,^\circ$ phase drop at each nodal position of the amplitude measurement. The phase accuracy is mainly defined by the spatial resolution of the measurement method, which itself is defined by the capacitive interaction area (averaging) between the tip apex and the DUT. This has been identified as 2 µm for the model-based measurement method [21]. Since the variation of the phase on the line occurs on a much larger length scale, the phase drop at the respective locations can be correctly measured. In agreement with the analytic calculation, the phase transition in the 26.5 GHz measurement also becomes less steep for lower position values (at -6.2 mm) than for the position closest to the open end (at -1.2 mm). This shows the influence of damping depending on the position along the line. The results verify the wide bandwidth amplitude and phase voltage measurement capability of the implemented method.

Although the measurement results closely match the calculated voltage along the line, there are deviations at certain positions x (for example in the amplitude at -2.5 mm for the 26.5 GHz measurement). For a further analysis, a RF voltage map across a short section of the matched line in Fig. 5 is recorded at 26.5 GHz with a position resolution of 2 µm. The map is shown in Fig. 11a. Fig. 11b shows the mean value of the 10 positions x in Fig. 11a and the error bars denote the respective standard deviations. The cross-section shows the structure of the DUT, with a 50 µm wide center conductor and the ground planes at the left and right of the gaps. Steep transitions between the gaps and the center conductor demonstrate the

Published version of the article: Mathias Poik, Thomas Hackl, Stefano Di Martino, Bernhard M. Berger, Sebastian W. Sattler and Georg Schitter, "A contactless method for measuring amplitude and phase of RF voltages up to 26.5 GHz ", *IEEE Sensors Journal*, 2024. DOI: 10.1109/JSEN.2024.3354322

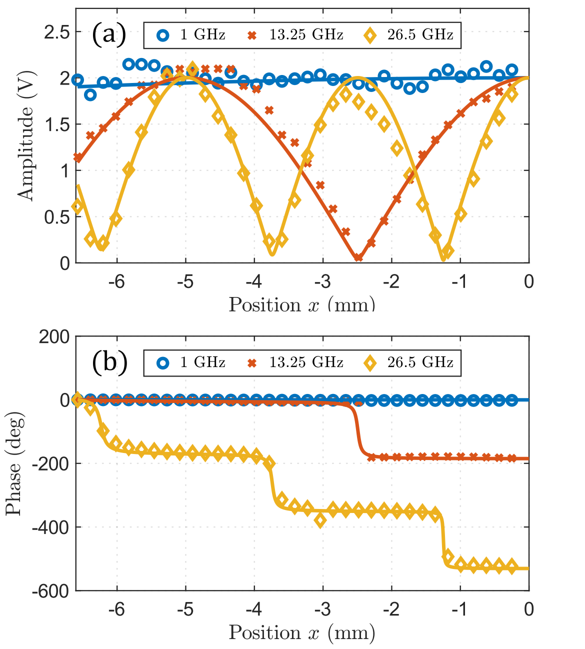

Fig. 10: (a) Amplitude and (b) phase of the measured RF voltage along the open-ended line (Figure 6) at different frequencies. The continuous lines show the analytical result based on (2).

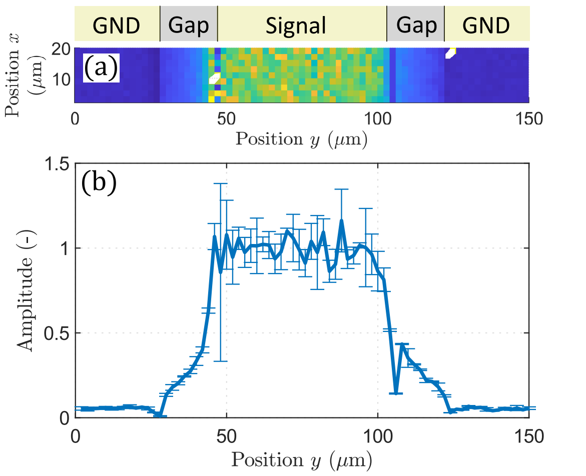

Fig. 11: Measured RF voltage amplitude across matched line at 26.5 GHz. (a) Voltage map of a 20 µm long line section. Bright color indicates higher amplitude. (b) Mean values and standard deviations of measured voltages in (a).

high spatial resolution of the probe, which has been reported in [22]. Although the measured RF voltage is roughly constant across the 50 µm wide center conductor, there are significant local fluctuations of the voltage. This may be explained by surface roughness of the metal conductors, which leads to minor variations of the identified tip-surface capacitance in the used measurement procedure and limits the accuracy of the measurement for this DUT. However, the purpose of this DUT is the verification of the wide bandwidth amplitude and phase sensing capability of the developed method. The target application is RF sensing within integrated microwave circuits, which are typically covered by thin, flat passivation layers, and should enable a better accuracy of the developed method [22].

In summary, it has been shown that the developed method enables amplitude and phase measurements of RF voltages at high spatial resolution and over a wide bandwidth from 1 GHz to 26.5 GHz.

VII. Conclusion

The proposed method enables amplitude and phase measurements of RF voltages at high spatial resolution over a wide bandwidth. A previously reported model-based measurement procedure [21] for the compensation of cross-talk induced errors is generalized and extended to allow the contactless measurement of both amplitude and phase of RF voltages at µm spatial resolution. A passive voltage probe is developed, consisting of a cantilever probe with a sharp tip which is mounted to a transmission line. It is experimentally verified that capacitively detected RF signals can be transmitted to a VNA over a wide bandwidth from 1 GHz to 26.5 GHz. The developed method together with the wide-bandwidth probe are verified by performing measurements on an open-ended transmission line. Measured standing wave patterns along the line at 1 GHz, 13.25 GHz and 26.5 GHz closely match the theoretically expected results. Ongoing work is focused on the application of the developed RF sensing system for voltage measurements in integrated microwave circuits.

References

[1] A. Rumiantsev and R. Doerner, "RF Probe Technology: History and Selected Topics," *IEEE Microwave Magazine*, vol. 14, no. 7, pp. 46–58, 2013.

[2] A. Joseph, A. Botula, J. Slinkman, R. Wolf, R. Phelps, M. Abou-Khalil, J. Ellis-Monaghan, S. Moss, and M. Jaffe, "Power handling capability of an SOI RF switch," in *Digest of Papers - IEEE Radio Frequency Integrated Circuits Symposium*, 2013, pp. 385–388.

[3] D. Denis, C. M. Snowden, and I. C. Hunter, "Coupled Electrothermal, Electromagnetic, and Physical Modeling of Microwave Power FETs," *IEEE Transactions on Microwave Theory and Techniques*, vol. 54, no. 6, pp. 2465–2470, 2006.

[4] V. Solomko, O. Oezdamar, R. Weigel, and A. Hagelauer, "Model of Substrate Capacitance of MOSFET RF Switch Inspired by Inverted Microstrip Line," in *ESSDERC 2021 - IEEE 51st European Solid-State Device Research Conference (ESSDERC)*, Sep. 2021, pp. 207–210.

[5] O. Oezdamar, A. Hagelauer, R. Weigel, and V. Solomko, "An RF Voltage Detector with Low Harmonic Feedback for Antenna Tuning Switches," in *2019 IEEE International Conference on Microwaves, Antennas, Communications and Electronic Systems (COMCAS)*, 2019, pp. 1–5.

[6] R. G. Venter, R. Hou, K. Buisman, M. Spirito, K. Werner, and L. C. de Vreede, "A package-integratable six-port reflectometer for power devices," in *2014 IEEE MTT-S International Microwave Symposium (IMS2014)*. IEEE, 2014, pp. 1–4.

[7] R. Hou, M. Spirito, R. Heeres, F. Van Rijs, and L. C. De Vreede, "Non-intrusive near-field characterization of distributed effects in large-periphery LDMOS RF power transistors," *2015 IEEE MTT-S International Microwave Symposium, IMS 2015*, pp. 1–3, 2015.

Published version of the article: Mathias Poik, Thomas Hackl, Stefano Di Martino, Bernhard M. Berger, Sebastian W. Sattler and Georg Schitter, "A contactless method for measuring amplitude and phase of RF voltages up to 26.5 GHz", *IEEE Sensors Journal*, 2024. DOI: 10.1109/JSEN.2024.3354322

This article has been accepted for publication in IEEE Sensors Journal. This is the author's version which has not been fully edited and content may change prior to final publication. Citation information: DOI 10.1109/JSEN.2024.3354322

[8] W. Fang, H. Qiu, C. Luo, L. Wang, W. Shao, E. Shao, S. Li, and Y. En, "Noncontact RF Voltage Sensing of a Printed Trace via a Capacitive-Coupled Probe," *IEEE Sensors Journal*, vol. 18, no. 21, pp. 8873–8882, 2018.

[9] N. Dehghan and S. C. Cripps, "A novel in-situ calibration technique for a high resolution E-Field probe," in *2015 IEEE MTT-S International Microwave Symposium*. IEEE, 2015.

[10] R. Hou, M. Lorenzini, M. Spirito, T. Roedle, F. van Rijs, and L. C. N. de Vreede, "Nonintrusive Near-Field Characterization of Spatially Distributed Effects in Large-Periphery High-Power GaN HEMTs," *IEEE Transactions on Microwave Theory and Techniques*, vol. 64, no. 11, pp. 4048–4062, 2016.

[11] N. Dehghan, "High Resolution Electric Field Probes with Applications in High Efficiency RF Power Amplifier Design," Dissertation, Cardiff University, 2014.

[12] D. Baudry, A. Louis, and B. Mazari, "Characterization of the Open-Ended Coaxial Probe Used for Near-Field Measurements in Emc Applications," *Progress In Electromagnetics Research*, vol. 60, pp. 311–333, 2006.

[13] R. Kantor and I. V. Shvets, "Measurement of electric-field intensities using scanning near-field microwave microscopy," *IEEE Transactions on Microwave Theory and Techniques*, vol. 51, no. 11, pp. 2228–2234, 2003.

[14] J. Wang, Z. Yan, W. Liu, X. Yan, and J. Fan, "Improved-Sensitivity Resonant Electric-Field Probes Based on Planar Spiral Stripline and Rectangular Plate Structure," *IEEE Transactions on Instrumentation and Measurement*, vol. 68, no. 3, pp. 882–894, 2019.

[15] W. Shao, W. Fang, Y. Huang, G. Li, L. Wang, Z. He, E. Shao, Y. Guo, Y. En, and B. Yao, "Simultaneous Measurement of Electric and Magnetic Fields With a Dual Probe for Efficient Near-Field Scanning," *IEEE Transactions on Antennas and Propagation*, vol. 67, no. 4, pp. 2859–2864, Apr. 2019.

[16] Z. Xin, X. Liu, X. Li, and J. Kang, "An Electric Field Probe With High Immunity for SiC MOSFET Switching Voltage Measurement," *IEEE Sensors Journal*, vol. 23, no. 7, pp. 7008–7016, 2023.

[17] G. Li, W. Shao, R. Chen, X. Tian, Q. Huang, X. Y. Zhang, W. Fang, and Y. Chen, "Ultrawideband Differential Magnetic Near Field Probe With High Electric Field Suppression," *IEEE Sensors Journal*, vol. 20, no. 14, pp. 7669–7676, 2020.

[18] S. Xue, S. Yang, W. Shao, X. Tian, and D.-l. Wu, "Electric Field Probe De-Embedding Calibration Based on Through and Line Standards," *IEEE Sensors Journal*, vol. 23, no. 7, pp. 6999–7007, 2023.

[19] G. Meyer and N. M. Amer, "Erratum: Novel optical approach to atomic force microscopy," *Applied Physics Letters*, vol. 53, no. 24, pp. 2400–2402, 1988.

[20] G. Gramse, M. Kasper, L. Fumagalli, G. Gomila, P. Hinterdorfer, and F. Kienberger, "Calibrated complex impedance and permittivity measurements with scanning microwave microscopy," *Nanotechnology*, vol. 25, no. 14, 2014.

[21] M. Poik, T. Hackl, S. Di Martino, M. Schober, J. Dang, and G. Schitter, "Model-Based RF Sensing for Contactless High Resolution Voltage Measurements," *IEEE Transactions on Instrumentation and Measurement*, pp. 1–1, 2023.

[22] ——, "Analysis of Cross-Talk Induced Measurement Errors in Model-Based RF Voltage Sensing," in *2023 IEEE International Instrumentation and Measurement Technology Conference (I2MTC)*, May 2023, pp. 1–6.

[23] S. Jarrix, T. Dubois, R. Adam, P. Nouvel, B. Azais, and D. Gasquet, "Probe characterization for electromagnetic near-field studies," *IEEE Transactions on Instrumentation and Measurement*, vol. 59, no. 2, pp. 292–300, 2010.

[24] K. Beilenhoff, H. Klingbeil, W. Heinrich, and H. L. Hartnagel, "Open and short circuits in coplanar mmic's," *IEEE Transactions on microwave theory and techniques*, vol. 41, no. 9, pp. 1534–1537, 1993.

[25] L. Fumagalli, G. Ferrari, M. Sampietro, I. Casuso, E. Martinez, J. Samitier, and G. Gomila, "Nanoscale capacitance imaging with attofarad resolution using ac current sensing atomic force microscopy," *Nanotechnology*, vol. 17, no. 18, pp. 4581–4587, 2006.

Published version of the article: Mathias Poik, Thomas Hackl, Stefano Di Martino, Bernhard M. Berger, Sebastian W. Sattler and Georg Schitter, "A contactless method for measuring amplitude and phase of RF voltages up to 26.5 GHz ", *IEEE Sensors Journal*, 2024. DOI: 10.1109/JSEN.2024.3354322